

# Green Chemistry

Accepted Manuscript



This article can be cited before page numbers have been issued, to do this please use: A. Rosengren, S. J. Butler, M. Arcos-Hernandez, K. Bergquist, P. Jannasch and H. Stålbrand, *Green Chem.*, 2019, DOI: 10.1039/C8GC03947J.



This is an Accepted Manuscript, which has been through the Royal Society of Chemistry peer review process and has been accepted for publication.

Accepted Manuscripts are published online shortly after acceptance, before technical editing, formatting and proof reading. Using this free service, authors can make their results available to the community, in citable form, before we publish the edited article. We will replace this Accepted Manuscript with the edited and formatted Advance Article as soon as it is available.

You can find more information about Accepted Manuscripts in the [author guidelines](#).

Please note that technical editing may introduce minor changes to the text and/or graphics, which may alter content. The journal's standard [Terms & Conditions](#) and the ethical guidelines, outlined in our [author and reviewer resource centre](#), still apply. In no event shall the Royal Society of Chemistry be held responsible for any errors or omissions in this Accepted Manuscript or any consequences arising from the use of any information it contains.

# Enzymatic synthesis and polymerisation of $\beta$ -mannosyl acrylates produced from renewable hemicellulosic glycans

View Article Online  
DOI: 10.1039/C9GC03947J

Anna Rosengren<sup>1a</sup>, Samuel J. Butler<sup>1a</sup>, Monica Arcos-Hernandez<sup>b</sup>, Karl-Erik Bergquist<sup>b</sup>, Patric Jannasch<sup>b</sup>, Henrik Stålbrand<sup>a\*</sup>

<sup>1</sup>These authors contributed equally to the study

<sup>a</sup>Department of Biochemistry and Structural Biology, Department of Chemistry, Lund University, PO Box 124, S-221 00 Lund, Sweden.

<sup>b</sup>Centre for Analysis and Synthesis, Department of Chemistry, Lund University, PO Box 124, S-221 00 Lund, Sweden

\*E-mail: Henrik.Stalbrand@biochemistry.lu.se, Tel: +46-46-222 8202, Fax: +46-46-222 4116

## Abstract

We show that glycoside hydrolases can catalyse the synthesis of glycosyl acrylate monomers using renewable hemicellulose as glycosyl donor, and we also demonstrate the preparation of novel glycopolymers by radical polymerisation of these monomers. For this, two family 5  $\beta$ -mannanases (*TrMan5A* from *Trichoderma reesei* and *AnMan5B* from *Aspergillus niger*) were evaluated for transglycosylation capacity using 2-hydroxyethyl methacrylate (HEMA) as glycosyl acceptor. Both enzymes catalysed conjugation between manno-oligosaccharides and HEMA, as analysed with MALDI-ToF mass spectrometry (MS) as initial product screening method. The two enzymes gave different product profiles (glycosyl donor length) with HEMA, as well as with allyl alcohol as acceptor molecules. *AnMan5A* appeared to prefer saccharide acceptors with lower intensity MS peaks detected for the desired allyl and HEMA conjugations. Contrary to *AnMan5A*, *TrMan5A* gave pronounced MS peaks for HEMA-saccharide conjugation products. *TrMan5A* was shown to catalyse the synthesis of  $\beta$ -mannosyl acrylates using locust bean gum galactomannan or softwood hemicellulose (acetyl-galactoglucomannan) as donor substrate. Evaluation of reaction conditions using galactomannan as donor, HEMA as acceptor and *TrMan5A* as enzyme catalyst was followed by the enzymatic production and preparative liquid chromatography purification of 2-( $\beta$ -manno(oligo)syloxy) ethyl methacrylates (Mannosyl-EMA and Mannobiosyl-EMA). The chemical structures and radical polymerisations of these novel monomers were concluded using <sup>1</sup>H and <sup>13</sup>C NMR spectroscopy and size-exclusion chromatography. The two new water soluble polymers have a polyacrylate backbone with one or two pendant mannosyl groups per monomeric EMA unit, respectively. These novel glycopolymers may show properties suitable for various technical and biomedical applications responding to the current demand for functional greener materials to replace fossil based ones.



## Introduction

Significant research efforts are currently devoted to establishing novel routes for the utilisation of major renewable resources in the form of plant biomass. The major motivation is to replace fossil resources in the production of energy, chemicals and materials. Glycans build up the major part of plants, of which hemicellulose constitute a large hitherto unused resource<sup>1</sup>. Simultaneously there is an increased interest to utilise defined glycan moieties in novel glycopolymer structures, in which the backbone carries pendant saccharide groups<sup>2</sup>. Here the term glycopolymer refers to polymers synthesised by the polymerisation of glycomonomers which are saccharides conjugated to a reactive group, such as for example acrylates.

By attachment of functional groups to saccharides, creating functionalised glycomonomers, novel glycopolymers can be synthesised, e.g., through thiol-ene click chemistry or radical polymerisation<sup>3-6</sup>. The polar carbohydrate groups in glycopolymers can be expected to facilitate water solubility and decrease backbone association. Many application areas can be foreseen and examples include colloidal stabilisers and coatings<sup>7</sup>. The glycan moieties in glycopolymers can also provide powerful biological recognition for biomedical and biocontrol applications<sup>2</sup>.

The complexity of carbohydrate structures provides challenges in the synthesis of glycomonomers for polymerisation reactions. Synthesis of glycopolymers such as polyacrylates with pendant saccharides requires well defined saccharide acrylate monomers as starting materials. The chemical synthesis of such glycomonomers is very demanding and includes multiple protection and deprotection steps<sup>8</sup>. There is an increasing interest in utilising enzymatic synthesis for these applications. Enzymatic synthesis is a greener alternative compared to chemical synthesis<sup>9</sup>. Advantages of enzymatic synthesis include high specificity, operation at ambient temperature, avoiding harsh chemicals and toxic by-products<sup>10</sup>. Furthermore, regio- and stereo-selective synthesis of glycoconjugates can be achieved with enzyme catalysis, without several steps of protection chemistry<sup>11</sup>. These advantages make it attractive to use renewable and abundant glycans as glycosyl donor substrates in enzyme catalysed reactions with functional glycosyl acceptors. Such reactions result in novel reactive glycomonomers, which in turn can be polymerised into glycopolymers. Glycoside hydrolases (GHs) with the retaining mechanism are of particular interest since they may, in addition to bond cleavage, catalyse the synthesis of new glycoside bonds via kinetically controlled transglycosylation<sup>12-14</sup> (Scheme 1). During the reaction, the glycosyl donor substrate is conjugated with a glycosyl acceptor. The reactive part of the acceptor is a hydroxyl group and alcohols can be used in the synthesis of alkyl glycosides (green surfactants)<sup>13, 15</sup>.

A few studies on enzymatic synthesis of glucosyl acrylates, catalysed by amylases or  $\beta$ -glucosidases, with starch<sup>5</sup> or cellobiose<sup>16</sup> as donor substrates have previously been reported. In this study we investigate the possibility of using abundant and renewable  $\beta$ -mannan as donor substrate for synthesis of mannosyl acrylates. There are different types of polymeric  $\beta$ -mannans (Scheme 2). Galactomannan is found in plant seeds in the form of industrially applied locust bean gum (LBG) and the more complex polysaccharide *O*-acetyl galactoglucomannan (AcGGM) is the main hemicellulose in softwoods<sup>1</sup>. Constituting up to 25% of the dry wood weight, AcGGM is a major renewable resource which can be obtained from forest industry waste streams<sup>17-19</sup>.

Among the enzymes responsible for efficient degradation of AcGGM and other  $\beta$ -mannans are the GH family 5  $\beta$ -mannanases.  $\beta$ -Mannanases catalyse cleavage of  $\beta$ -mannans and due to their retaining



catalytic mechanism they may have ability to catalyse transglycosylation, i.e. the synthesis of  $\beta$ -mannosidic bonds, fusing donor saccharides and acceptor molecules as described above. This can be utilised for enzymatic synthesis of novel glycoconjugates. The active site of  $\beta$ -mannanases is often located in a cleft where two catalytic amino acids are situated. During the catalytic event, a covalent intermediate is formed between the enzyme and the saccharide. This intermediate is then disrupted by either a water molecule (in hydrolysis) or another acceptor molecule (in transglycosylation), the latter leading to synthesis of a new glycoconjugate (Scheme 1). We have previously shown that the  $\beta$ -mannanase *TrMan5A* from *Trichoderma reesei* possesses the ability to perform transglycosylation, linking donor mannosides to various acceptor alcohols<sup>20-22</sup>. We have also previously studied the synthetic capacity of  $\beta$ -mannanases from *Aspergillus nidulans* and found one  $\beta$ -mannanase; *AnMan5B*, with exceptionally high transglycosylation capacity with saccharide acceptors compared to other  $\beta$ -mannanases<sup>21</sup>.

Here we expand our previous approaches on enzymatic synthesis, with a focus on investigating the potential use of a polymerisable acceptor molecule; hydroxyethyl methacrylate (HEMA) (Scheme 1B) in transglycosylation reactions with  $\beta$ -mannanases (*TrMan5A* and *AnMan5B*) and different  $\beta$ -mannans. The primary aim is to produce novel mannosyl acrylates to be used as glycomonomers in polymerisation reactions.

This research supports the potential for finding a biotechnological route for using renewable mannans as starting materials for enzymatic synthesis of novel functional building blocks for preparation of glycopolymers. AcGGM is indeed an interesting renewable resource with great potential, and we show that it can act as donor substrate for enzymatic synthesis of mannosyl acrylates. However, in this first study of enzymatic synthesis of mannosyl acrylates we choose to use the less complex and commercially available LBG as donor substrate in scaled up synthetic reactions. Enzymatic reactions with *TrMan5A*, LBG and HEMA generated the least heterogenic product profile. Through  $\beta$ -mannanase catalysed transglycosylation, two mannosyl acrylate monomers were produced. These were purified in sufficient amounts to allow for structural determination by NMR spectroscopy, and their respective homopolymers were prepared in conventional radical polymerisations.



## Experimental

View Article Online  
DOI: 10.1039/C8GC03947J

### Materials

Azo-carob galactomannan, low viscosity carob (locust bean gum) galactomannan (LBG) with a mannose:galactose ratio of 1:0.28, mannobiose ( $M_2$ ), mannotriose ( $M_3$ ), mannotetraose ( $M_4$ ), mannopentaose ( $M_5$ ) and mannohexaose ( $M_6$ ) were supplied by Megazyme (Bray, Ireland). Locust bean gum galactomannan with a mannose:galactose ratio of 1:0.25 was from Sigma-Aldrich (St. Louis, MO, USA). Dextran (50 kDa, 150 kDa, 270 kDa, 410 kDa and 1400 kDa) was from Fluka Chemie AG (Buchs, Switzerland). *O*-Acetyl galactoglucomannan (AcGGM) was prepared and analysed according to Lundqvist *et al.*<sup>17</sup> (average molecular weight of 5900 Da and molar monomer composition, mannose: glucose: galactose: acetyl being 1: 0.4: 0.15: 0.7). Mannose ( $M_1$ ) (microbiology grade), sodium acetate (molecular biology grade), acetic acid, 2-hydroxyethyl methacrylate (HEMA) 97% containing 200 ppm hydroquinone (HQ), 2,5-dihydroxy benzoic acid (DHB), hydroquinone (HQ,  $\geq 99\%$ ), diethyl ether ( $\geq 97\%$ ) containing 1 ppm BHT as inhibitor, ethanol, butanol, acetonitrile (ACN, anhydrous 99.9%, HPLC gradient grade), *N*-(1-naphtyl) ethylenediamine dihydrochloride, sulphuric acid, ammonium persulphate (APS), and potassium disulfite were all obtained from Sigma-Aldrich (St. Louis, MO, USA). All aqueous solutions were prepared with MilliQ water.

### $\beta$ -Mannanases

*Trichoderma reesei* Man5A (*TrMan5A*) was obtained by production in *Trichoderma reesei* as described previously<sup>23</sup>. An aliquot of freeze-dried enzyme powder was dissolved in 50 mM Na-acetate buffer pH 5.3. The solution was thrice centrifuged and refilled with buffer in Vivaspin columns with 10 kDa cut-off (Sartorius, Göttingen, Germany). *Aspergillus nidulans* Man5B (*AnMan5B*) was expressed in *Pichia pastoris* and purified as previously reported<sup>21</sup>. Protein concentration was determined by measuring the absorbance at 280 nm and using the extinction coefficient 123145  $M^{-1} cm^{-1}$  for *TrMan5A* and 118510  $M^{-1} cm^{-1}$  for *AnMan5B*, calculated using ProtParam (<http://web.expasy.org/protparam/>).

### Enzymatic reactions with $M_4$ and HEMA or allyl alcohol

Reactions were set up with either *TrMan5A* or *AnMan5B* (2  $\mu M$ ), mannotetraose ( $M_4$ ) (5 mM) as glycosyl donor substrate and either HEMA (25 vol%) or allyl alcohol (25 vol%) as glycosyl acceptor (Scheme 1), in 20 mM Na-acetate buffer pH 5.3. Total reaction volume was 50  $\mu L$ . Incubation was done in sealed 0.2 ml PCR tubes at 37  $^{\circ}C$ , samples (10  $\mu L$ ) were taken at 5 min, 1, 3 and 5 h and reactions were terminated by boiling 5 min, after which no enzyme activity remained.

### Matrix-assisted laser desorption ionisation - time of flight mass spectrometry (MALDI-ToF MS)

MALDI-ToF MS was used for analysis of reactions with oligosaccharide and polysaccharide donor substrates incubated with the acceptor and either *TrMan5A* or *AnMan5B*. Samples (0.5  $\mu L$ ) were co-crystallised with 0.5  $\mu L$  DHB (10  $g L^{-1}$  in  $H_2O$ ) on a stainless steel MALDI plate, using warm air to dry the spots. MALDI-ToF MS data was collected using a MALDI-ToF 4700 (Applied Biosystems) in positive reflector mode. In general, a laser intensity of 5500-6000 was used and 20 sub spectra with 50 shots/spectrum were collected from each sample spot. The software "Data Explorer version 4.5" was



used for analysis of mass spectrometry data. MALDI-ToF-ToF MS/MS data was collected in positive mode with a laser intensity of 6500, a precursor window of  $\pm 0.100$  Da and collecting 75 sub spectra with 15 shots/spectrum for each sample spot.

View Article Online  
DOI: 10.1039/C8GC03947J

### Thin layer chromatography

For reactions with *TrMan5A* and HEMA, samples were also analysed on thin layer chromatography (TLC) using aluminium plates covered with silica gel 60 (Merck, Darmstadt, Germany). 1  $\mu$ L of manno-oligosaccharide standards ( $M_1$ - $M_6$ , 10 mM) and 2  $\mu$ L of samples were loaded on the plate. A mobile phase of butanol-ethanol-water in volume ratio 10:8:7 was used for separation for about 8 h at room temperature. Visualisation of sugars was done by soaking the plate in a solution containing *N*-(1-naphthyl) ethylenediamine dihydrochloride, ethanol and sulphuric acid<sup>24</sup> followed by drying and incubation at 105 °C for 10 min.

### Determination of retained $\beta$ -mannanase activity in aqueous HEMA solution

*TrMan5A* was incubated at 37 °C in aqueous solutions of HEMA ranging 0-25 vol%. Analysis of residual enzyme activity was performed at 0, 1, 5 and 24 h (for 20% HEMA also at 48h). For analysis of  $\beta$ -mannanase activity, an assay with azo-carob galactomannan was used. The assay was performed according to recommendations from the manufacturer (Megazyme, Bray, Ireland).

### Enzymatic reactions with polymeric $\beta$ -mannan and HEMA

To assess the ability of *TrMan5A* to use HEMA as acceptor in reactions with polysaccharides, locust bean gum galactomannan (LBG, Sigma-Aldrich) was firstly tested as glycosyl donor substrate. Initial reactions (50  $\mu$ L) were set up with *TrMan5A* (2  $\mu$ M), LBG (Sigma-Aldrich) (0.25% (w/v)) and HEMA (0-25 vol%) in 30 mM Na-acetate buffer pH 5.3. Samples were incubated at 37 °C for 24 h, followed by boiling 5 min to terminate the reactions. The more complex polysaccharide AcGGM (Scheme 2) was also tested as glycosyl donor substrate in reactions with HEMA as glycosyl acceptor. The spruce AcGGM was extracted and analysed according to Lundqvist *et al.*<sup>17</sup> An aliquot of freeze dried AcGGM was dissolved in milliQ water. Reactions (50  $\mu$ L) were performed with *TrMan5A* (2  $\mu$ M) and AcGGM (0.35% (w/v)) in 20 mM Na-acetate buffer pH 5.3 with or without HEMA (25 vol%). Incubation was done at 37 °C for 24 h followed by 5 min boiling to terminate the reactions. These initial reactions with polysaccharide substrates were analysed with MALDI-ToF MS.

To assess the effect of different reaction parameters on the synthesis of mannosyl acrylates, time-course studies were carried out on reactions with *TrMan5A* (0.2-2  $\mu$ M), LBG (Megazyme) (0.25-3% (w/v)) and HEMA (10-20 vol%) in 30 mM Na-acetate buffer pH 5.3. Incubation was done at 37 °C for up to 48 h. Sample aliquots were collected after <5min, 0.5 h, 1 h, 2 h, 5 h, 8 h, 24 h and 48 h, terminating the reaction through boiling for 5 min. Reactions with 2  $\mu$ M *TrMan5A* were terminated after 24 h, whilst reactions with 0.2  $\mu$ M *TrMan5A* were terminated after 48 h. Reaction volumes ranged 0.75-5 ml and the impact of altered reaction parameters was evaluated by HPLC analysis (see below).





## HPLC analysis

View Article Online  
DOI: 10.1039/C8GC03947J

After initial screening for products using MALDI-ToF MS, as described above, samples were analysed by HPLC. Unreacted HEMA was partially extracted with diethyl ether, to diminish void peak and allow for accurate HPLC analysis of the analytes. Equal volumes of reaction sample and diethyl ether were mixed thoroughly, the organic phase was removed, and the extraction was performed three times. Prior to injection on the column, samples were diluted with ACN to be compatible with the starting conditions for the HPLC analysis. Samples from 0.25-1% (w/v) LBG incubations were diluted 1:1 in ACN, whilst samples from 2-3% (w/v) LBG incubations were diluted 1:3 in ACN. All samples were filtered through a 0.2  $\mu\text{m}$  polytetrafluoroethylene (PTFE) filter prior to loading. An Ultimate 3000 system from Thermo Scientific was used for HPLC analysis. Data was collected using UV-detection at 205 nm, which has previously been used for detection of glucosyl acrylates<sup>5</sup>. Samples were run on a  $\text{NH}_2$  column (LUNA amino, 250x4.6 mm, 3  $\mu\text{m}$ , Phenomenex, Torrance, CA, USA) using hydrophilic interaction liquid chromatography (HILIC) conditions.  $\text{H}_2\text{O}$  and ACN were used as mobile phase at 1 ml min<sup>-1</sup>. A gradient from 5-60%  $\text{H}_2\text{O}$  over 30 min was used for separation. The column was then washed with 90%  $\text{H}_2\text{O}$  for 10 min followed by equilibration at 5%  $\text{H}_2\text{O}$  for 10 min. The injection volume was 10  $\mu\text{l}$  and the column temperature was maintained at 40 °C. Fractions of eluting peaks were collected and analysed by MALDI-ToF MS and MS/MS, as described above.

## Preparative scale production of 2-( $\beta$ -manno(oligo)syloxy) ethyl methacrylates ( $\text{M}_n\text{EMAs}$ )

Based on detected product peak areas from the HPLC analysis, reaction conditions that gave the largest product peak areas of 2-( $\beta$ -mannosyloxy) ethyl methacrylate ( $\text{M}_1\text{EMA}$ ) and 2-( $\beta$ -mannobiosyloxy) ethyl methacrylate ( $\text{M}_2\text{EMA}$ ) were chosen for preparative production of these compounds. In a total reaction volume of 50 ml, 0.2  $\mu\text{M}$  *TrMan5A* was incubated with 3% LBG (w/v) (Megazyme) and 20 vol% HEMA in 30 mM sodium acetate buffer pH 5.3, for 48 h at 37 °C. The reaction vessels were occasionally mixed through inversion, to ensure homogenous conditions. Unreacted HEMA was extracted three times with diethyl ether, in a volume proportion of 1:1. The organic phase was discarded. 50  $\mu\text{l}$  of the polymerisation inhibitor HQ (10 g L<sup>-1</sup>), was added to the remaining, aqueous fraction, which was then concentrated in an RVC 2-18 SpeedVac (Martin Christ Gefriertrocknungsanlagen GmbH, Osterode am Harz, Germany) maintaining temperatures <40 °C. To condition the sample for preparative HPLC, the resulting concentrated syrup (~2.5 ml) was diluted first in 2.5 ml  $\text{H}_2\text{O}$  and then in increments of ACN to a final concentration of 95% ACN. The incremental increase of ACN precipitated saccharide moieties with DP>3 (as analysed with MALDI-ToF MS), which were separated from the soluble fraction, by decantation and filtration, before loading the sample onto the HPLC column.

## Preparative HPLC purification of $\text{M}_n\text{EMAs}$

Preparative HPLC was performed with a preparative HPLC system (2545 Quaternary gradient module, 2707 Autosampler, Fraction collector III, Prep degasser, 2998 Photodiode array detector and Column oven) (Waters, Milford, MA, USA). UV-data was collected at 205 nm. Prior to loading samples were filtered through a 0.2  $\mu\text{m}$  PTFE filter. Samples, equivalent to 22.5 ml of the original reaction volume, in 95% ACN, were purified using a preparative  $\text{NH}_2$  column (LUNA 5  $\mu\text{m}$   $\text{NH}_2$  100 Å, 250x21.2 mm AXIA packed, Phenomenex, Torrance, CA, USA) using HILIC conditions. Samples were loaded during isocratic conditions of 5%  $\text{H}_2\text{O}$  in ACN, and eluted during gradient flow, with increasing concentration of  $\text{H}_2\text{O}$ , up to 60%. Elution fractions were collected in 8 ml polypropylene fraction collection tubes. The column



was washed with 90% ACN:H<sub>2</sub>O before re-equilibration with three column volumes at the starting conditions. The flow rate was constant at 20 ml min<sup>-1</sup>, and column temperature was maintained at 40 °C.

The fractions collected from the preparative scale purification were thoroughly analysed by MALDI-ToF MS, MS/MS and analytical HPLC, as described above. The concentration in aliquots of purified M<sub>1</sub>EMA and M<sub>2</sub>EMA was determined by nuclear magnetic resonance (NMR) spectroscopy with external reference, by using an optimised tuning and matching approach for comparison between two samples. A sample with known concentration of HEMA was used as external standard. The quantified samples were further used to construct external standard curves, allowing for quantification of M<sub>n</sub>EMAs via HPLC analysis.

Fractions containing the major products, M<sub>1</sub>EMA and M<sub>2</sub>EMA, were pooled and supplemented with 6 µg of HQ as inhibitor. The respective product was concentrated in a SpeedVac maintaining temperatures <40 °C. The M<sub>1</sub>EMA was concentrated to a visually clear, slightly viscous solution <50 µl, and the M<sub>2</sub>EMA was concentrated to a brownish syrup <20 µl. The two samples were then resuspended in 500-550 µl D<sub>2</sub>O (99.8%), centrifuged at 15000 g for 10 min at room temperature to remove any particulates, and the supernatants were transferred to new tubes prior to NMR analyses.

### Analysis by NMR spectroscopy

The purified fractions of M<sub>1</sub>EMA and M<sub>2</sub>EMA, and eventually their corresponding individual polymers, were used for structural analysis by NMR spectroscopy. <sup>1</sup>H and <sup>13</sup>C spectra were recorded at 10 and 45 °C on a Bruker Avance III spectrometer (Bruker, Billerica, MA, USA) at 500.17 MHz for <sup>1</sup>H and at 125.77 MHz for <sup>13</sup>C. Chemical shift assignment was made using two dimensional NMR experiments; <sup>1</sup>H correlation spectroscopy (COSY), total correlation spectroscopy (TOCSY), heteronuclear multiple-bond correlation (HMBC), heteronuclear single quantum coherence (HSQC) NMR and 2D nuclear Overhauser effect spectroscopy (NOESY) with 800 ms mixing time. Chemical shifts for the proton spectra (δ<sub>H</sub>) were given in ppm relative to the residual internal solvent peak taking into account the temperature dependence<sup>25</sup> (HDO, δ<sub>H</sub> 4.94 ppm at 10 °C and δ<sub>H</sub> 4.55 for 45 °C). <sup>13</sup>C spectra chemical shift scale was obtained using Bruker software Topspin 3.2 pl6 for calculating the unified scale according to the International Union of Pure and applied Chemistry (IUPAC)<sup>26</sup>. The chosen temperatures for spectra acquisition were different to room temperature in order to induce a shift of the residual internal solvent (HDO) to reveal or improve the resolution of the anomeric signals arising from the mannose units. Additionally, coupled <sup>13</sup>C spectra were obtained at 125.77 MHz at 10 °C in D<sub>2</sub>O with a gated decoupling technique to study the direct coupling constant between C-1 and H-1 (<sup>1</sup>J<sub>C-1,H-1</sub>).

### Polymerisation

Conventional radical polymerisations of the M<sub>1</sub>EMA and M<sub>2</sub>EMA monomers were carried out using K<sub>2</sub>S<sub>2</sub>O<sub>5</sub> and APS as initiator system in a threaded capped NMR tube at a molar monomer to K<sub>2</sub>S<sub>2</sub>O<sub>5</sub> to APS ratio of 100:4:17, and at a monomer concentration of 30 mM in D<sub>2</sub>O. The reaction solution was purged by bubbling nitrogen through a syringe for 1 h at room temperature. The polymerisation reaction was then carried out at 60 °C during 24 h under nitrogen atmosphere. Subsequently, the tube was left to cool to room temperature, followed by immediate acquisition of <sup>1</sup>H and <sup>13</sup>C NMR spectra to confirm the polymerisation. Once the polymerisation was confirmed, the samples were further





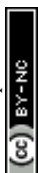
analysed by size exclusion chromatography (SEC). A sample volume of 20  $\mu\text{l}$  (1 mg  $\text{ml}^{-1}$ ) was injected on a TSKgel® G4000PW<sub>XL</sub> column (TOSOH Bioscience GmbH, Griesheim, Germany) connected to a chromatography system (Waters 600E System Controller, Waters, Milford, MA, USA), using RI (Waters 2414 Differential Refractometer) and UV detection (Waters 486 Tunable Absorbance Detector) at 234 nm. De-ionized water served as eluent at a flow rate of 0.5  $\text{ml min}^{-1}$ . The column was calibrated with dextran standards of 50, 150, 270, 410, and 1400 kDa (Fluka Chemie AG, Buchs, Switzerland). The remaining volume of the samples was diluted with  $\text{D}_2\text{O}$  followed by acquisition of  $^1\text{H}$  and  $^{13}\text{C}$  NMR spectra at 10 and 45  $^\circ\text{C}$ .

**2-( $\beta$ -mannosyloxy) ethyl methacrylate,  $\text{M}_1\text{EMA}$ :**  $^1\text{H}$  NMR ( $\text{D}_2\text{O}$ , 10  $^\circ\text{C}$ )  $\delta_{\text{H}}$  in ppm, chemical shift scale from residual HDO ( $\delta$  4.94): 6.14 (H-e, br), 5.71 (H-e, br), 4.72 (H-1, s), 4.33- 4.38 (H-b, m), 4.12 (H-a, m), 3.97 (H-2, dd), 3.94 (H-a, m), 3.90 (H-6, dd), 3.70 (H-6, dd), Impurity (3.64, s), 3.61 (H-3, dd), 3.54 (H-4, t), 3.35 (H-5, m), 2.70 (Impurity, s), 2.03 (Impurity, s), 1.92 (H-f, s).

$^{13}\text{C}$  NMR ( $\text{D}_2\text{O}$ , 10  $^\circ\text{C}$ )  $\delta_{\text{C}}$  in ppm, chemical shift scale from the unified scale according to IUPAC<sup>26</sup>: 169.73 (C-c), 135.76 (C-d), 126.99 (C-e), 99.92 (C-1), 76.31 (C-5), 72.91 (C-3), 70.45 (C-2), 67.31 (C-a), 66.75 (C-4), 64.29 (C-b), 62.49 (Impurity), 61.02 (C-6), 38.65 (Impurity), 17.43 (C-f).

**2-( $\beta$ -mannobiosyloxy) ethyl methacrylate,  $\text{M}_2\text{EMA}$ :**  $^1\text{H}$  NMR ( $\text{D}_2\text{O}$ , 10  $^\circ\text{C}$ )  $\delta$  in ppm, chemical shift scale from residual HDO ( $\delta$  4.94): 6.15 (H-e, br), 5.71 (H-e, br), 4.74 (H-1, s), 4.72 (H-1', s), 4.33- 4.38 (H-b, m), 4.12 (H-a, m), 4.04 (H-2', d), 4.03 (H-2, d), 3.97 (H-a, m), 3.93 (H-6', dd), 3.87 (H-6, dd), ~3.80 (H-4, q), 3.77 (H-3, dd), 3.73 (H-6, dd), 3.70 (H-6', dd), 3.63 (H-3', dd), 3.53 (H-4', dd), 3.47 (H-5, m), 3.42 (H-5', m), 3.33 (Impurity), 3.18 (Impurity, q), 2.70 (Impurity, s), 2.04 (Impurity, s), 1.91 (H-f, s), 1.26 (Impurity, t), 1.14 (Impurity, d).

$^{13}\text{C}$  NMR ( $\text{D}_2\text{O}$ , 10  $^\circ\text{C}$ )  $\delta$  in ppm, chemical shift scale from the unified scale according to IUPAC<sup>26</sup>: 169.73 (C-c), 135.75 (C-d), 127.01 (C-e), 100.22 (C-1'), 99.94 (C-1), 76.76 (C-4), 76.43 (C-5'), 74.88 (C-5), 72.72 (C-3'), 71.61 (C-3), 70.50 (C-2'), 69.84 (C-2), 67.38 (C-a), 66.68 (C-4'), 64.31 (C-b), 61 (C-6), 60.52 (C-6'), 38.65 (Impurity), 17.44 (C-f).



## Results and discussion

View Article Online  
DOI: 10.1039/C8GC03947J

### Reactions with mannotetraose ( $M_4$ ) as donor substrate and HEMA as acceptor

*TrMan5A* has previously been shown to have synthetic capacity via transglycosylation when incubated with  $M_4$  as glycosyl donor substrate and alcohols such as methanol, butanol and hexanol as glycosyl acceptors<sup>21, 22</sup>. *AnMan5B*, however, does not use methanol or butanol as acceptors in reactions with  $M_4$ <sup>21</sup>. On the other hand, *AnMan5B* displays exceptionally high transglycosylation capacity with saccharide acceptors and even seems to prefer saccharides over water<sup>21</sup>. To investigate whether *TrMan5A* and *AnMan5B* can synthesise glycoconjugates by using HEMA as acceptor (Scheme 1), initial reactions were set up with  $M_4$  as donor substrate. Reactions with allyl alcohol as acceptor were included for comparison (Scheme 1C).

In a first screening, samples from the enzymatic reactions with  $M_4$ , HEMA or allyl alcohol were analysed with MALDI-ToF mass spectrometry. For *TrMan5A*, peaks corresponding to masses of molecules generated by a conjugation between manno-oligosaccharides and allyl alcohol (Fig. 1A) or manno-oligosaccharides and HEMA (Fig. 1D) were detected, further referred to as "conjugates". Also for *AnMan5B*, peaks corresponding to masses of conjugates with both allyl alcohol and HEMA were detected (Fig. 1B and C) but at a lower peak intensity compared to *TrMan5A*. In addition, *AnMan5B* also generated significant transglycosylation products with saccharides as acceptors, in agreement to what has previously been reported<sup>21</sup>. In the reactions with *AnMan5B* and allyl alcohol, the only detected conjugate peak was allyl-mannobioside ( $M_2$ -allyl) (Fig. 1B), showing an intensity that was significantly lower compared to the  $M_2$ -allyl peak detected in the *TrMan5A* reactions. In reactions with *AnMan5B* and HEMA, low intensity peaks corresponding to masses of conjugates with up to six mannosyl units were detected (Fig. 1C).

Based on the complexity and heterogeneity of the product profile generated by *AnMan5B*, together with lower peak intensity for the conjugates compared to the *TrMan5A* reactions, the enzyme chosen for further studies was *TrMan5A*. HEMA was selected as acceptor for further study, as the polymerisation of saccharide acrylates can be demonstrated without the need for co-monomers<sup>4-6</sup>.

In the MS spectra of reactions with *TrMan5A*,  $M_4$  and HEMA (Fig. 1D), peaks corresponding to masses of manno-oligosaccharides as well as of conjugations between mannose and HEMA; 2-( $\beta$ -mannosyloxy) ethyl methacrylate ( $M_1$ EMA), mannobiose and HEMA; 2-( $\beta$ -mannobiosyloxy) ethyl methacrylate ( $M_2$ EMA) and mannotriose and HEMA; 2-( $\beta$ -mannotriosyloxy) ethyl methacrylate ( $M_3$ EMA) were detected (Fig. 1D). MALDI-ToF-ToF MS/MS analysis of the peaks corresponding to  $M_2$ EMA and  $M_3$ EMA further supported that they originated from mannosyls conjugated with HEMA (Fig. 1E). The MS/MS spectra gave Y and B ions that could be matched to the  $M_2$ EMA and  $M_3$ EMA fragmenting in the glycosidic bond (Fig. 1E)<sup>27, 28</sup>.

A TLC analysis of reactions with *TrMan5A*,  $M_4$  and HEMA also showed that the enzymatic reaction generated, in addition to oligosaccharides, products that migrated further on the plate compared to oligosaccharide standards (Fig. S1), i.e. products that were less hydrophilic than oligosaccharides. These products were assumed to be conjugates with HEMA. None of the controls (substrate, enzyme and HEMA control) showed spots at the same level on the plate. A previously reported TLC analysis of reactions with  $M_4$  and *TrMan5A* indicated no spots migrating further than mannose<sup>21</sup>. The combined results from the MALDI-ToF MS and TLC analysis showed that the *TrMan5A*  $\beta$ -mannanase can use HEMA as acceptor in reactions with  $M_4$  as donor substrate, to generate 2-( $\beta$ -manno(oligo)syloxy) ethyl



methacrylates ( $M_n$ EMAs), and that the  $M_n$ EMAs can be separated from manno-oligosaccharides based on differences in hydrophilicity.

HPLC analysis of the reaction with *Tr*Man5A,  $M_4$  and HEMA, separated on an  $NH_2$  column run in HILIC conditions, resulted in separation of three clear peaks (Fig. 1F). Fractions were collected and elutes were identified by MALDI-ToF MS, as the conjugates;  $M_1$ EMA,  $M_2$ EMA and  $M_3$ EMA. The MS analysis verified that the peaks in the HPLC chromatogram each contained one conjugate and no other conjugate or saccharide.

### Assessment of reactions with polymeric mannans and HEMA

The experiments with  $M_4$  gave valuable insights on both enzymatic performance and the setup of analytical procedures. The interesting finding that *Tr*Man5A can synthesise  $M_n$ EMAs when incubated with  $M_4$  as donor substrate, and that these can be separated on a HPLC column, provided promising results when moving on to set up reactions using polymeric mannans, LBG and AcGGM, as donor substrates. To our knowledge these abundant and naturally occurring mannans have previously not been evaluated as donor substrates in enzymatic synthesis reactions.

In MALDI-ToF MS analysis of reactions with LBG and HEMA, conjugates between HEMA and hexoses up to degree of polymerisation (DP) 3 were detected (Fig. S2 B), together with non-conjugated oligosaccharide products of DP2-4, also present in the reactions without HEMA (Fig. S2 A). In addition, samples from reactions with LBG and HEMA were analysed on HPLC, and peaks with the same retention times as previously determined for  $M_1$ - $M_3$ EMA were detected. This concluded that *Tr*Man5A can synthesise  $M_n$ EMAs also when using LBG as donor substrate.

As a first trial towards using a renewable resource from the forest industry as donor substrate, AcGGM extracted from spruce<sup>17</sup>, was also evaluated in enzymatic reactions with HEMA. MALDI-ToF MS analysis of these reactions gave more complex spectra due to the higher complexity of the AcGGM substrate compared to LBG (Fig. S2 C, D). Spectra from reactions, both with and without HEMA, showed peaks corresponding to hexoses with DP1-7 (H1-H7) (Fig S2 C, D). Since the AcGGM substrate is partly acetylated<sup>17</sup>, oligosaccharides of hexoses with one, two or three acetyl groups were present (Fig S2 C, D). In the reactions where HEMA was included, peaks that correspond to masses of conjugates between HEMA and hexoses up to DP4 were detected (Fig. S2 D). Both non-acetylated and acetylated conjugates with HEMA were detected in the spectra (Fig. S2 D). Although the results from reactions with AcGGM provide novel and promising results, the commercially available donor substrate LBG was chosen for further reactions in this study, due to limited amount of available AcGGM and in order to limit product heterogeneity.

### Enzyme stability

Analysis of the stability of *Tr*Man5A in various HEMA concentrations was performed to refine the reaction conditions for the synthesis of  $M_n$ EMAs. The results from the stability analysis of *Tr*Man5A are presented in Fig 2. *Tr*Man5A is stable at 37 °C for 24 h without presence of HEMA. Also, with 5 and 10 vol% HEMA the enzyme maintained its activity after incubation for 5 h, and after 24 h at these concentrations of HEMA the remaining activity was 85-90%. With 15 and 20 vol% HEMA the enzyme was stable for 1 h and the activity then decreased to 85% and 65% respectively after 5 h, and to 60% and 35%, respectively, after 24 h. With 25 vol% HEMA the enzyme maintained around 85% of its activity for 1 h. Then the activity decreased to 40% after 5 h, and became negligible after 24 h. With



concentrations of up to 20 vol% HEMA, *TrMan5A* is operational for at least 24 h at 37 °C and therefore this concentration of HEMA and this temperature was chosen for further reactions. A prolonged incubation under this condition (20% HEMA, 37°C) showed that *TrMan5A* had lost all activity after 48h.

### Reaction parameters

In order to obtain amounts of  $M_n$ EMAs that allowed further characterisation, the effect of varying different reaction parameters on the synthesis of  $M_n$ EMAs was investigated. Time-course studies over 0-48 h were set up, altering donor substrate and acceptor concentrations and enzyme load, respectively. Based on detectable peak areas from HPLC analysis of the conjugates, the various conditions were evaluated (Fig. 3). Using the same amount of enzyme (2  $\mu$ M *TrMan5A*), whilst increasing the donor substrate concentration (0.25-3% (w/v) LBG) and acceptor concentration (10 vol% vs 20 vol% HEMA) resulted in higher HPLC peak area of the  $M_n$ EMA products, where  $M_2$ EMA gave the largest peaks (Fig. 3A). The highest product formation was obtained at 3% LBG and 20% HEMA (25% less  $M_2$ EMA was detected using 10% HEMA). The  $M_2$ EMA detection using 1% or 0.25% LBG instead of 3%, decreased by 39% and 87%, respectively. The reaction progression over time using 3% LBG and 20% HEMA revealed a decrease of the  $M_2$ EMA after prolonged incubation (34% less detected at 24h compared to 2h) (Fig. 3B). The peak response of  $M_1$ EMA, however, increased steadily over the time course (Fig. 3B). The decrease in  $M_2$ EMA levels could potentially be caused by secondary hydrolysis<sup>13</sup>. Such hydrolysis of the terminal mannosyl unit would also explain the increasing levels of  $M_1$ EMA. With a lower enzyme load (0.2  $\mu$ M rather than 2  $\mu$ M) secondary hydrolysis appeared to be limited and the maximum amounts of conjugates, based on HPLC peak areas, were obtained after a 48 h incubation of 0.2  $\mu$ M *TrMan5A* with 3% (w/v) LBG and 20 vol% HEMA.

In order for the observed secondary hydrolysis to occur, the  $M_2$ EMA molecule needs to be able to bind in the active site-cleft of *TrMan5A* through subsites -1, +1 and +2 with the two mannoses in subsites -1 and +1, to expose the target terminal glycosidic bond for the catalytic amino acids<sup>29</sup>. This would also mean that the EMA moiety can be accommodated in the +2 subsite which is an important site for glycan interactions both in hydrolysis and transglycosylation<sup>20</sup>. Furthermore, for the synthesis of  $M_n$ EMAs shown in the current paper to occur, HEMA needs to be accommodated in subsite +1 to be positioned for conjugation with the mannosyl in subsite -1. The picture emerges that the EMA unit can replace mannosyl units in this type of enzyme-ligand interactions within distal subsites (i.e. not -1). This view is also supported by the interesting observation that mannanase *AnMan5B* uses HEMA as acceptor (Fig. 1C), but not shorter alcohols<sup>21</sup>. Interaction or accommodation of EMA units in this type of enzymes potentially opens up for further reactions involving this chemical group and enzyme catalysis.

### Preparative production of $M_n$ EMA

Based on the reaction conditions that gave the highest amount of  $M_n$ EMA products, reactions were set up in 50 ml scale. These conditions were deduced from peak area on analytical HPLC and resulted in the use of 0.2  $\mu$ M *TrMan5A*, 3% (w/v) LBG and 20 vol% HEMA, incubated for 48 h. Separation of  $M_n$ EMA products was performed with preparative HPLC by collecting and further analysing the fractions (Fig. 4). To determine purity of the fractions collected from the preparative HPLC run, each



fraction was analysed by MALDI-ToF MS (Fig. 4); the fractions were determined to be free from sugars and only contain one type of  $M_n$ EMA. The  $M_n$ EMA peaks were further studied by MALDI-ToF-ToF MS/MS, revealing a fragmentation pattern corroborating the identity of each peak (data not shown).

The sample concentrations, analysed with NMR, were determined to be 11.5 g L<sup>-1</sup> (in 500  $\mu$ l) for  $M_1$ EMA and 20.2 g L<sup>-1</sup> (in 540  $\mu$ l) for  $M_2$ EMA. These quantified samples were then used as external standards in HPLC analysis for quantification of  $M_n$ EMAs in different reactions.

### Reaction yields

The concentration of  $M_n$ EMAs in the preparative scale (50 ml) reactions was quantified to 0.306 g L<sup>-1</sup> ( $\pm$  0.008)  $M_1$ EMA and 0.953 g L<sup>-1</sup> ( $\pm$  0.009)  $M_2$ EMA, corresponding to a yield of 3.63% ( $\pm$ 0.026) (Table 1). The yield was calculated based on mannosyl units in the conjugates ( $M_1$ EMA and  $M_2$ EMA) vs mannosyl units in the donor substrate (LBG, with the theoretical amount of galactose subtracted). It can be noted that when, in the smaller scale, using lower concentrations of LBG as donor substrate (0.25-1% (w/v)) (Fig. 3A), the yield was higher (6.52% ( $\pm$ 0.22) and 7.42% ( $\pm$ 0.64) respectively), but the reactions resulted in lower concentration of conjugates. The lower yield in reactions with higher LBG concentration could potentially be due to the increased viscosity of the donor substrate, which may cause diffusion limitations. These reactions were also incubated longer, which may have led to partial loss of enzyme activity during the reaction time. Using  $M_4$  as donor substrate (Fig. 1C) resulted in higher yield (13.8% ( $\pm$  1.0)) compared to when using the more complex LBG as donor substrate (Table 1). This yield is comparable with the yield obtained in reactions where cellobiose was used a donor substrate in enzymatic synthesis of glucosyl-methacrylamide monomers (12-18%)<sup>16</sup>, although higher concentrations of both donor substrate and acceptor was used in that study. A strong point in our approach is that unmodified natural glycans can be used as donors, rather than activated (para-nitrophenyl or nucleotide) sugars which likely results in higher rates and yields<sup>16</sup>.

Interestingly, the obtained yield for synthesis of  $M_2$ EMA using  $M_4$  as donor substrate was about 12 times higher compared to synthesis of hexyl mannobioside, also using *TrMan5A* and similar concentrations and conditions<sup>22</sup>. Although, the limited water solubility of hexanol likely plays a role, the potentially favourable accommodation or interaction of HEMA in the *TrMan5A* active site cleft (as discussed above) can be an additional positive factor.

The drastic difference in yield between the more complex LBG and the oligosaccharide  $M_4$  indicates that pre-hydrolysis of the target substrate may result in higher reaction efficacy. Pre-hydrolysis would generate shorter saccharides and also decrease the viscosity of the donor substrate, which could favour the enzymatic synthesis. The approach with pre-hydrolysis has previously been used and applied for enzymatic synthesis of alkyl-glycosides, using insoluble ivory nut mannan as starting material<sup>22</sup>. Additional strategies to improve the yield in reactions with mannans could be to remove side groups. Galactose substitutions along the main back bone of the galactomannan substrate may cause steric hindrance for the  $\beta$ -mannanase and limit productive binding<sup>30</sup>. Thus, a synergistic hydrolysis of galactose residues, by the action of an  $\alpha$ -galactosidase<sup>31</sup>, could enable further action on the substrate by the  $\beta$ -mannanase<sup>30, 32</sup> and improve yield.

### Structural analysis of the synthesised conjugates $M_1$ EMA and $M_2$ EMA

The *TrMan5A*  $\beta$ -mannanase uses the retaining double-displacement mechanism and is thus unequivocally expected to produce  $\beta$ -anomeric transglycosylation products<sup>12, 33</sup>. With this knowledge





and the MALDI-ToF MS mass determination of purified compounds we can predict their chemical structures, as 2-( $\beta$ -mannosyloxy) ethyl methacrylate ( $M_1$ EMA) and 2-( $\beta$ -mannobiosyloxy) ethyl methacrylate ( $M_2$ EMA) (Fig. 5).

The structure of  $M_2$ EMA was fully resolved by NMR spectroscopy. The  $^1\text{H}$  and  $^{13}\text{C}$  spectra for  $M_2$ EMA can be seen in Fig. 6 and Fig. S3, respectively. Wholly resolved  $^1\text{H}$  and  $^{13}\text{C}$  spectra of  $M_2$ EMA, showing the crowded "sugar region", can be found in supplementary figures Fig. S4 and S5. The structural determination was carried out by first comparing the spectra with published data, and then the assignment of signals was made unequivocally based on empirical rules for chemical shifts, coupling constants, multiplicity analysis and integration coupled with 2D NMR spectra analysis<sup>34</sup>. The use of 2D NMR techniques enables full assignment without relying on analogy with reference data<sup>35</sup>.

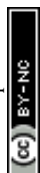
When analysing the  $M_2$ EMA sample, two different signals were identified in the anomeric region ( $\delta_{\text{H}}$  4.4-5.5<sup>2</sup> ppm) corresponding to the anomeric protons of the two mannoside units (H-1 and H-1' in Fig. 5B). The chemical shifts ( $\delta$  in ppm) were observed at 4.74 and 4.72 ppm respectively (Fig. 6). These values are in very good agreement with previously analysed internal and terminal non-reducing  $\beta$ -mannosyls of  $\beta$ -manno-oligosaccharides (4.72-4.75 ppm)<sup>33, 36</sup>, while non-reducing  $\beta$ -mannosyls or  $\beta$ -galactosyls of oligosaccharides display higher values (5.0-5.2 ppm)<sup>36, 37</sup>. Apart from these well separated signals arising from the anomeric protons, Fig. 6 shows a multitude of signals assigned as the 'sugar region' in  $\delta_{\text{H}}$  ~4.06-3.38 ppm and are in agreement with previously reported ranges for mannose based mono- and disaccharides, including methylated ones<sup>37</sup>.

In the next step the signals associated with the acrylate unit, in particular the signals corresponding to the acrylate double bond (H-e in Fig. 5), were observed at  $\delta_{\text{H}}$  6.14 and 5.71 ppm and those associated to the  $-\text{CH}_3$  protons (H-f in Fig. 5) at  $\delta_{\text{H}}$  1.92 ppm. These are in agreement with previously reported values at 5.70-6.14 ppm for H-e and at 1.87-1.91 ppm for H-f respectively<sup>38</sup>. They were also shown to be in agreement with the signals observed in spectra recorded from 2-hydroxyethyl methacrylate used for the synthesis ( $\text{D}_2\text{O}$ , 25 °C). The empirical assignment was in agreement with the initial assignment. Fig. 7 shows the overlapping of HMBC and HSQC spectra of  $M_2$ EMA, identifying relevant cross peaks that confirm the synthesis of the compound against the proposed structure (Fig. 5B). This data reveals the formation of the glycosidic linkage between the acrylate and the mannose unit at the anomeric carbon position (C-a to C-1 to C-2), as well as the linkage between the two mannose units (C-4 to C-1' to C-2'). As no other chemical shifts showed such correlations in the overlapped 2D spectra, we confirm the formation of these linkages. We further confirmed that no signal can be found that would correspond to the presence of (1 $\rightarrow$ 6)-linked  $\alpha$ -D-galactopyranosyl units.

We also confirmed that the synthesised  $M_1$ EMA corresponded to the proposed structure (Fig. 5A). Fig. S8 reveals the formation of the glycosidic linkage between the acrylate and the mannose unit at the anomeric carbon (C-a to C-1 to C-2), in analogy to the analysis in Fig. 7. Fully resolved  $^1\text{H}$  and  $^{13}\text{C}$  spectra for this compound can be found in supplementary information (Fig. S9-S10).

### Configuration at the anomeric carbon

The direct coupling constant  $^1J_{\text{C-1,H-1}}$  is the most reliable indication of anomeric configuration<sup>34</sup>. It has been reported that this coupling constant in pyranose derivatives of carbohydrates is approximately 10 Hz lower for an axial ( $\beta$ ) H-1 compared to an equatorial H-1 ( $\alpha$ ), 160 Hz against 170 Hz respectively. This difference is found even when there are differences in the magnitudes related to the electronegativity of the substituent at C-1<sup>39</sup>. In both our samples this direct coupling constant,  $^1J_{\text{C-1,H-1}}$ , was determined to be ~160 Hz, which is in agreement with the observed in pyranose derivatives for





an axial ( $\beta$ ) H-1 (Fig. S6). As an additional confirmation of the  $\beta$ -configuration, we observed strong NOE between H-1 (anomeric proton) and H2, H3 and H5 in  $M_1$ EMA, which has been observed for  $\beta$ -D-mannose<sup>35</sup> (Fig. S7). We hereby conclude that the resolved structure of enzymatically synthesised  $M_2$ EMA corresponds to the hypothesised molecular structure (Fig. 5B).

## Polymerisation of the enzymatically produced monomers

### Poly( $M_1$ EMA) and poly( $M_2$ EMA)

The reactivity and polymerisability of the enzymatically synthesised mannosyl acrylate monomers were assessed by carrying out conventional thermally initiated radical polymerisations in  $D_2O$  at 60 °C during 24 h. Analysis of the products demonstrated that the synthesised glycomonomers ( $M_1$ EMA and  $M_2$ EMA) are readily polymerisable and form high molecular weight glycopolymers. The  $^1H$  spectrum of poly(2-( $\beta$ -mannobiosyloxy) ethyl methacrylate) (poly( $M_2$ EMA)) recorded at 45 °C (Fig. 8) showed the typical broadening of signals due to the different chemical environments of the repeating units along the polymer chain. The  $-CH_2-$  group (H-E) of the polymer backbone appeared in the region 1.5 – 2.5 ppm. The broadening at 0.8 – 1.2 ppm corresponds to the  $-CH_3$  group (H-F) which shifts down field upon polymerisation. As expected, the signals corresponding to the double bond of the  $-CH_2$  group (H-e) of the acrylate group in the monomer disappeared after polymerisation (Fig. 8). Kloosterman and co-workers observed the same changes upon polymerisation of 2-( $\beta$ -glucosyloxy) ethyl methacrylate<sup>5</sup>. The  $^1H$  spectra of poly(2-( $\beta$ -mannosyloxy) ethyl methacrylate) (poly( $M_1$ EMA)) also revealed the reactive nature of these monomers (data not shown).

The polymerisation solutions were also analysed by SEC (Fig. 9). The main peak of poly( $M_2$ EMA) eluted with the void (5.2 ml). The main peak of poly( $M_1$ EMA) eluted at 6 ml, which corresponds to an apparent molecular weight larger than the highest dextran standard included (dextran 1400 kDa, elution volume 6.7 ml). It should be noted that both poly( $M_2$ EMA) and poly( $M_1$ EMA) showed additional minor peaks in the SEC chromatogram. For poly( $M_2$ EMA), a peak eluting at 7.4 ml (close to the elution volume for dextran 410 kDa) was seen. For poly( $M_1$ EMA) a minor peak eluted at 9.5 ml, which is later than the smallest dextran standard used (dextran 50 kDa eluted at 8.8 ml). In comparison, a standard of polyethylene glycol (PEG) of 400 Da eluted at 11.5 ml. Based on the present data, it is not possible to conclude whether the synthesised polymers form aggregates, which could potentially be the reason why multiple peaks were present in the SEC analysis. However, the SEC data further confirmed that the enzymatic synthesis of polymerisable monomers was successful, resulting in novel glycopolymers. Further study of these glycopolymers is an interesting future perspective but it is out of the scope of this study.

Glycopolymers such as the ones prepared in our study are of great interest as they can be produced from renewable abundant carbohydrate sources. Glycopolymers based on acrylate monomers have received particular attention due to their multiple potential applications<sup>2, 40-42</sup>. Acrylates and methacrylates are extensively used in industry because they are highly versatile and can be polymerised or copolymerised with numerous monomers to tune material properties. They can be used to produce functional materials that range from soft rubbers to non-film forming materials<sup>43</sup>. By attaching a glycan structure to the acrylate functionality, yielding our glycomonomers, we expect to contribute to further functional versatility. Through different polymerisation techniques we may increase the possibilities for new applications. For example, we envision to synthesise a range of novel polymers with different properties via copolymerisation with different comonomers. The glycan part will then likely modulate solubility and aggregation properties, and also potentially contribute with



specific affinity for biomaterial surfaces and tissues, further widening the applications in biomaterial technology and biomedicine.

View Article Online

DOI: 10.1039/C8GC03947J

## Conclusions

We have successfully demonstrated the enzyme catalysed synthesis of mannosyl acrylate monomers and their polymerisation into novel polyacrylates with one or two pendant mannosyl units. We show that the choice of  $\beta$ -mannanase used for synthesis is important since different product profiles were obtained with the two tested enzymes.  $\beta$ -Mannanase *AnMan5A* generated longer saccharide conjugates compared to *TrMan5A* with  $M_4$  as donor and either HEMA or allyl alcohol as acceptor. These product profiles are in good agreement with previous transglycosylation reactions using saccharides or simpler alcohols as acceptors<sup>21</sup>. We furthermore demonstrate that abundant and renewable hemicellulosic  $\beta$ -mannans (locust bean galactomannan and softwood hemicellulose) can directly be used as donor glycans in the  $\beta$ -mannanase catalysed synthesis of these mannosyl acrylate monomers. Different conditions for reactions using  $\beta$ -mannanase *TrMan5A* as catalyst, locust bean gum galactomannan as donor and HEMA as acceptor were investigated. A 50 ml reaction generated sufficient amounts of HILIC purified  $M_1$ EMA and  $M_2$ EMA to verify the predicted chemical structure of these two novel glycomonomers, using  $^1\text{H}$  and  $^{13}\text{C}$  NMR spectroscopy.  $M_1$ EMA and  $M_2$ EMA polymerised into novel water soluble acrylic polymers carrying pendant mannosyl or mannobiosyl units, respectively. These pendant glycan moieties are expected to be evenly distributed along the polyacrylate chain and we believe that varying the ratio between them individually, as well as using other acrylate monomers during polymerisation, will enable the design of future glycopolymers with differences in properties such as solubility, aggregation and surface/biomolecular interaction.

The new monomers thus have the potential to open up for new applications, also taking advantage of the specific interaction of mannosyl units with biomolecules<sup>2</sup>. A route forward to reach such applications could, upscaling aside, involve increase of the yield during the enzymatic synthesis. An interesting approach there would be either pre-hydrolysis of the galactomannan<sup>22</sup> or enzyme synergy by the inclusion of a sidegroup cleaving enzyme. This could increase the exposure of the  $\beta$ -mannan backbone to the  $\beta$ -mannanase, which has been shown for other enzyme systems<sup>30</sup>. These two approaches would probably also aid when further investigating abundant forestry resources (AcGGM) as glycan donor, for which the first trials were made here.

It is also worth mentioning that different  $\beta$ -mannanases clearly yield different glycan length during synthesis. Hence, an increased understanding of the catalysts would aid in future enzyme development approaches to govern product profiles<sup>22</sup>, as well as limit secondary hydrolysis, further increasing the capability to synthesise defined acrylate glycomonomers. In the current paper, we also further establish mass spectrometry as a powerful tool for screening when conditions or enzyme variants are initially evaluated.



## Conflicts of interest

View Article Online  
DOI: 10.1039/C8GC03947J

The authors declare no conflicts of interest.

## Acknowledgements

This study was financed by the Swedish Foundation for Strategic Research (SSF) through grant RBP14-0046 and Carl Tryggers Stiftelse. We thank Eimantas Šileikis for technical help related to preparative HPLC. We are also grateful for the help and assistance of Dr. Christoffer Karlsson in the NMR analysis of the monomers.



## References

View Article Online  
DOI: 10.1039/C8GC03947J

1. H. V. Scheller and P. Ulvskov, in *Annu. Rev. Plant Biol.*, eds. S. Merchant, W. R. Briggs and D. Ort, 2010, vol. 61, pp. 263-289.
2. S. R. S. Ting, G. Chen and M. H. Stenzel, *Polym. Chem.*, 2010, **1**, 1392-1412.
3. A. B. Lowe, *Polym. Chem.*, 2010, **1**, 17-36.
4. M. Obata, M. Shimizu, T. Ohta, A. Matsushige, K. Iwai, S. Hirohara and M. Tanihara, *Polym. Chem.*, 2011, **2**, 651-658.
5. W. M. J. Kloosterman, D. Jovanovic, S. G. M. Brouwer and K. Loos, *Green Chem.*, 2014, **16**, 203-210.
6. W. M. J. Kloosterman, S. Roest, S. R. Priatna, E. Stavila and K. Loos, *Green Chem.*, 2014, **16**, 1837-1846.
7. S. Cheng, Y. Zhao and Y. Wu, *Prog. Org. Coat.*, 2018, **118**, 40-47.
8. M. Ambrosi, A. S. Batsanov, N. R. Cameron, B. G. Davis, J. A. K. Howard and R. Hunter, *J. Chem. Soc., Perkin Trans. 1*, 2002, 45-52.
9. J. J. Gridley and H. M. I. Osborn, *J. Chem. Soc., Perkin Trans. 1*, 2000, 1471-1491.
10. L. Wen, G. Edmunds, C. Gibbons, J. Zhang, M. R. Gadi, H. Zhu, J. Fang, X. Liu, Y. Kong and P. G. Wang, *Chem. Rev.*, 2018, **118**, 8151-8187.
11. T. J. Boltje, T. Buskas and G. J. Boons, *Nat. Chem.*, 2009, **1**, 611-622.
12. M. L. Sinnott, *Chem. Rev.*, 1990, **90**, 1171-1202.
13. F. van Rantwijk, M. W. V. Oosterom and R. A. Sheldon, *J. Mol. Catal. B: Enzym.*, 1999, **6**, 511-532.
14. P. Bojarova and V. Kren, *Trends Biotechnol.*, 2009, **27**, 199-209.
15. M. Ochs, M. Muzard, R. Plantier-Royon, B. Estrine and C. Rémond, *Green Chem.*, 2011, **13**, 2380-2388.
16. A. Adharis, D. Vesper, N. Koning and K. Loos, *Green Chem.*, 2018, **20**, 476-484.
17. J. Lundqvist, A. Jacobs, M. Palm, G. Zacchi, O. Dahlman and H. Stalbrand, *Carbohydr. Polym.*, 2003, **51**, 203-211.
18. S. Willfor, K. Sundberg, M. Tenkanen and B. Holmbom, *Carbohydr. Polym.*, 2008, **72**, 197-210.
19. A. Andersson, T. Persson, G. Zacchi, H. Stalbrand and A. S. Jonsson, *Appl. Biochem. Biotechnol.*, 2007, **137**, 971-983.
20. A. Rosengren, P. Hagglund, L. Anderson, P. Pavon-Orozco, R. Peterson-Wulff, W. Nerinckx and H. Stalbrand, *Biocatal. Biotransform.*, 2012, **30**, 338-352.
21. A. Rosengren, S. K. Reddy, J. S. Sjöberg, O. Aurelius, D. T. Logan, K. Kolenova and H. Stalbrand, *Appl. Microbiol. Biotechnol.*, 2014, **98**, 10091-10104.
22. J. Morrill, A. Manberger, A. Rosengren, P. Naidjonoka, P. von Freiesleben, K. Krogh, K. E. Bergquist, T. Nylander, E. N. Karlsson, P. Adlercreutz and H. Stalbrand, *Appl. Microbiol. Biotechnol.*, 2018, **102**, 5149-5163.
23. P. Hagglund, T. Eriksson, A. Collen, W. Nerinckx, M. Claeysens and H. Stalbrand, *J. Biotechnol.*, 2003, **101**, 37-48.
24. M. Bounias, *Anal. Biochem.*, 1980, **106**, 291-295.
25. H. E. Gottlieb, V. Kotlyar and A. Nudelman, *The Journal of Organic Chemistry*, 1997, **62**, 7512-7515.
26. R. K. Harris, E. D. Becker, S. M. De Menezes, P. Granger, R. E. Hoffman and K. W. Zilm, *Magn. Reson. Chem.*, 2008, **46**, 582-598.
27. B. Domon and C. E. Costello, *Glycoconjugate J.*, 1988, **5**, 397-409.
28. G. L. Sasaki and L. M. de Souza, in *Tandem Mass-spectrometry - Molecular Characterisation* 2013, ch. 4, pp. 82-115.



29. E. Sabini, H. Schubert, G. Murshudov, K. S. Wilson, M. Siika-Aho and M. Penttilä, *Acta Crystallogr D*, 2000, **56**, 3-13. View Article Online  
DOI: 10.1039/C8GC03947J
30. V. Bagenholm, S. K. Reddy, H. Bouraoui, J. Morrill, E. Kulcinskaja, C. M. Bahr, O. Aurelius, T. Rogers, Y. Xiao, D. T. Logan, E. C. Martens, N. M. Koropatkin and H. Stalbrand, *J. Biol. Chem.*, 2017, **292**, 229-243.
31. S. K. Reddy, V. Bagenholm, N. A. Pudlo, H. Bouraoui, N. M. Koropatkin, E. C. Martens and H. Stalbrand, *FEBS Lett.*, 2016, **590**, 2106-2118.
32. S. Malgas, J. S. van Dyk and B. I. Pletschke, *World J. Microbiol. Biotechnol.*, 2015, **31**, 1167-1175.
33. V. Harjunpaa, A. Teleman, M. Siika-Aho and T. Drakenberg, *Eur. J. Biochem.*, 1995, **234**, 278-283.
34. W. A. Bubba, *Concepts Magn. Reson., Part A*, 2003, **19A**, 1-19.
35. P. K. Agrawal, *Phytochemistry*, 1992, **31**, 3307-3330.
36. M. Tenkanen, M. Makkonen, M. Perttula, L. Viikari and A. Teleman, *J. Biotechnol.*, 1997, **57**, 191-204.
37. F. Pereira, *Carbohydr. Res.*, 2011, **346**, 960-972.
38. J. Voepel, J. Sjöberg, M. Reif, A.-C. Albertsson, U.-K. Hultin and U. Gasslander, *J. Appl. Polym. Sci.*, 2009, **112**, 2401-2412.
39. K. Bock and C. Pedersen, *J. Chem. Soc., Perkin Trans. 2*, 1974, 293-297.
40. S. Kitazawa, M. Okumura, K. Kinomura and T. Sakakibara, *Chem. Lett.*, 1990, **19**, 1733-1736.
41. M. Al-Bagoury, K. Buchholz and E.-J. Yaacoub, *Polym. Adv. Technol.*, 2007, **18**, 313-322.
42. M. Obata, R. Otobuchi, T. Kuroyanagi, M. Takahashi and S. Hirohara, *J. Polym. Sci., Part A-1: Polym. Chem.*, 2017, **55**, 395-403.
43. S. Srivastava, *Des. Monomers Polym.*, 2009, **12**, 1-18.



Table

View Article Online  
DOI: 10.1039/C8GC03947J

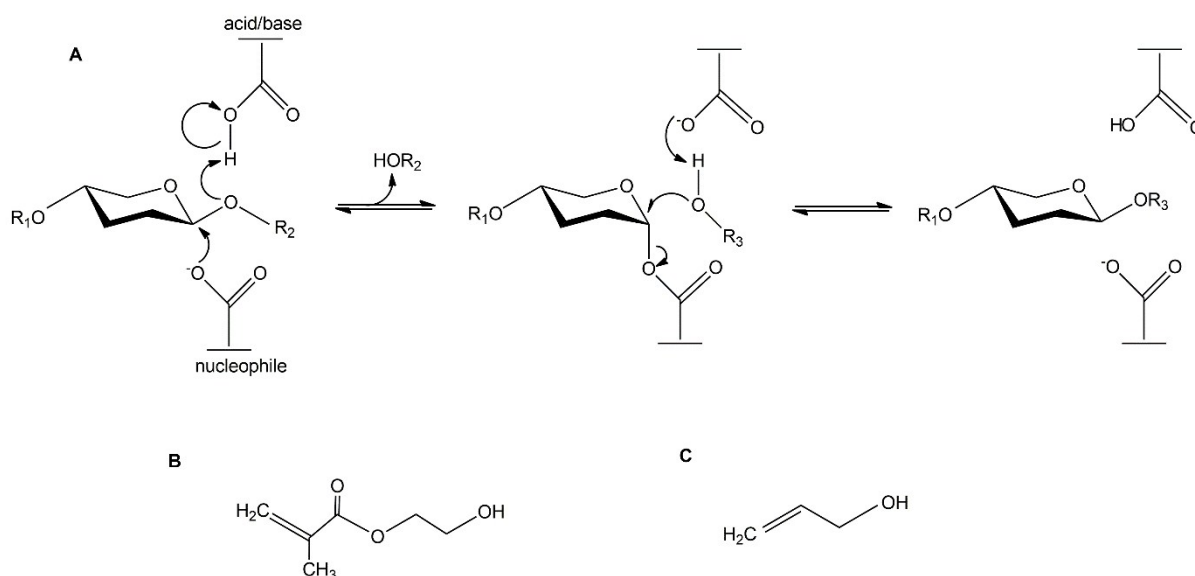
Table 1. Concentrations of M<sub>1</sub>EMA and M<sub>2</sub>EMA in *Tr*Man5A catalysed synthesis reactions, and calculated yield in % based on mannosyl units.

	M <sub>1</sub> EMA (g/L)	M <sub>2</sub> EMA (g/L)	Yield (%)	Enzyme concentration	Incubation time
M <sub>4</sub> 5 mM (0.33% (w/v))	0.106 (±0.003)	0.544 (±0.043)	13.78 (±1.0)	2 µM	1 h
LBG 0.25% (w/v)	0.036 (±0.005)	0.150 (±0.002)	6.52 (±0.22)	2 µM	1 h
LBG 1% (w/v)	0.202 (±0.029)	0.654 (±0.081)	7.42 (±0.54)	2 µM	1 h
LBG 3% (w/v)	0.306 (±0.008)	0.953 (±0.009)	3.63 (±0.026)	0.2 µM	48 h

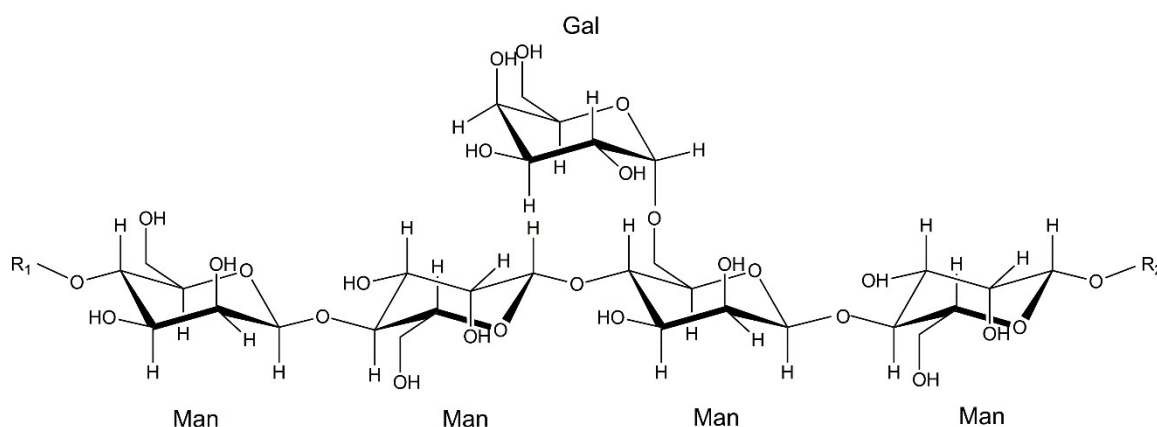




## Schemes

View Article Online  
DOI: 10.1039/C8GC03947J

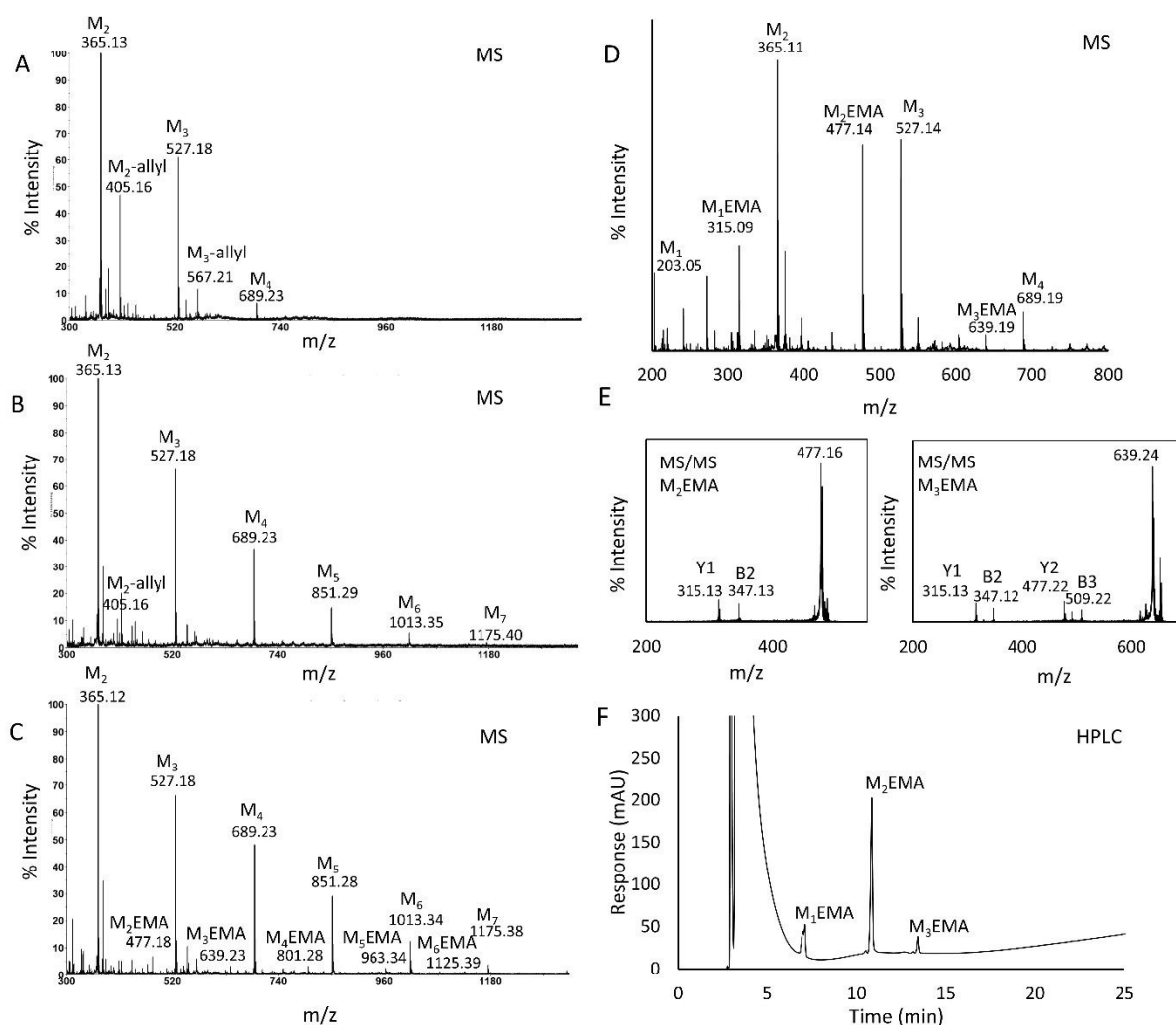
**Scheme 1. A)** Retaining mechanism of glycoside hydrolases.  $\text{R}_1$  and  $\text{R}_2$  represents the continuation of the saccharide chain.  $\text{R}_3$  represents the continuation of the acceptor molecule. The acceptor molecules used in this study are: **B)** 2-hydroxy ethyl methacrylate (HEMA) and **C)** allyl alcohol.



**Scheme 2.** Molecular structure of locust bean gum galactomannan (LBG) with a galactose: mannose ratio of 1:4. Man=mannose, Gal=galactose. In *O*-acetyl galactoglucomannan (AcGGM), the mannosyl units can be acetylated at positions C2 and C3 to various extent, and the polysaccharide backbone also contains glucose moieties.  $\text{R}_1$  and  $\text{R}_2$  represents the continuation of the glycan chain.



## Figures

View Article Online  
DOI: 10.1039/C8GC03947J

**Fig. 1.** Analysis of 1 h reactions with *TrMan5A* (2  $\mu$ M) or *AnMan5B* (2  $\mu$ M) using  $M_4$  (5 mM) as donor substrate and HEMA (25 vol%) or allyl alcohol (25 vol%) as acceptor. In MALDI-ToF MS (A-E), peaks were detected as monoisotopic masses of single charged sodium adducts. The theoretical  $m/z$  for the peaks corresponding to oligosaccharides and conjugates, marked in the figure, are:  $M_2$  ( $m/z$  365.11),  $M_3$  ( $m/z$  527.16),  $M_4$  ( $m/z$  689.21),  $M_5$  ( $m/z$  851.27),  $M_6$  ( $m/z$  1013.32),  $M_7$  ( $m/z$  1175.37),  $M_2$ -allyl ( $m/z$  405.14),  $M_3$ -allyl ( $m/z$  567.19),  $M_1$ EMA ( $m/z$  315.11),  $M_2$ EMA ( $m/z$  477.16),  $M_3$ EMA ( $m/z$  639.21),  $M_4$ EMA ( $m/z$  801.26),  $M_5$ EMA ( $m/z$  963.32) and  $M_6$ EMA ( $m/z$  1125.37).

**A)** MS spectra of the reaction with *TrMan5A*,  $M_4$  and allyl alcohol, showing the donor substrate  $M_4$ , oligosaccharide products  $M_2$  and  $M_3$  and peaks of conjugations between allyl alcohol and  $M_2$  and  $M_3$ ;  $M_2$ -allyl.

**B)** MS spectra of the reaction with *AnMan5B*,  $M_4$  and allyl alcohol, showing the donor substrate  $M_4$ , oligosaccharide products  $M_2$  and  $M_3$ , transglycosylation products  $M_5$ ,  $M_6$ ,  $M_7$  and a small peak of  $M_2$ -allyl.



**C)** MS spectra of the reaction with *An*Man5B, M<sub>4</sub> and HEMA, showing the donor substrate M<sub>4</sub>, oligosaccharide products M<sub>2</sub> and M<sub>3</sub>, transglycosylation products M<sub>5</sub>, M<sub>6</sub>, M<sub>7</sub> and small peaks of conjugations between HEMA and M<sub>2</sub>-M<sub>6</sub>; M<sub>2-6</sub>EMA. View Article Online  
DOI: 10.1039/C8GC03947J

**D)** MS spectra of the reaction with *Tr*Man5A, M<sub>4</sub> and HEMA, showing the donor substrate M<sub>4</sub>, oligosaccharide products M<sub>1</sub>, M<sub>2</sub> and M<sub>3</sub>, and peaks of conjugations between HEMA and M<sub>2</sub> and M<sub>3</sub>; M<sub>2-3</sub>EMA.

**E)** MS/MS fragmentation of M<sub>2</sub>EMA and M<sub>3</sub>EMA, showing Y1 and B2 ions for the M<sub>2</sub>EMA and Y1, Y2, B2 and B3 ions for the M<sub>3</sub>EMA, which were of expected m/z for molecules fragmenting in the glycosidic bond (theoretical m/z for Y1: 315.11, B2: 347.10, Y2: 477.16, B3: 509.12).

**F)** HPLC chromatogram showing separation of M<sub>1</sub>EMA, M<sub>2</sub>EMA and M<sub>3</sub>EMA. HPLC analysis was carried out with an analytical NH<sub>2</sub> column run under HILIC conditions. 10 µl sample (2x diluted) was injected. Three separate peaks were detected after the void: r<sub>f</sub> 1: 7.0 min, 2: 10.8 min and 3: 14.1 min. Fractions were collected and the peaks were individually identified as M<sub>1</sub>EMA, M<sub>2</sub>EMA and M<sub>3</sub>EMA respectively, by MALDI-ToF MS.



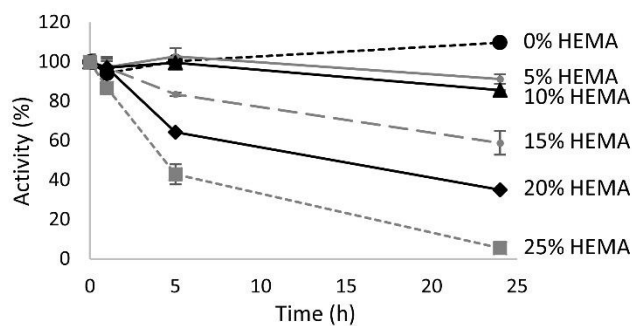


**Fig. 2.** Residual activity of *TrMan5A* in 0-25 vol% HEMA. Enzyme activity was analysed with an azo-carob galactomannan assay after 0-24 h.

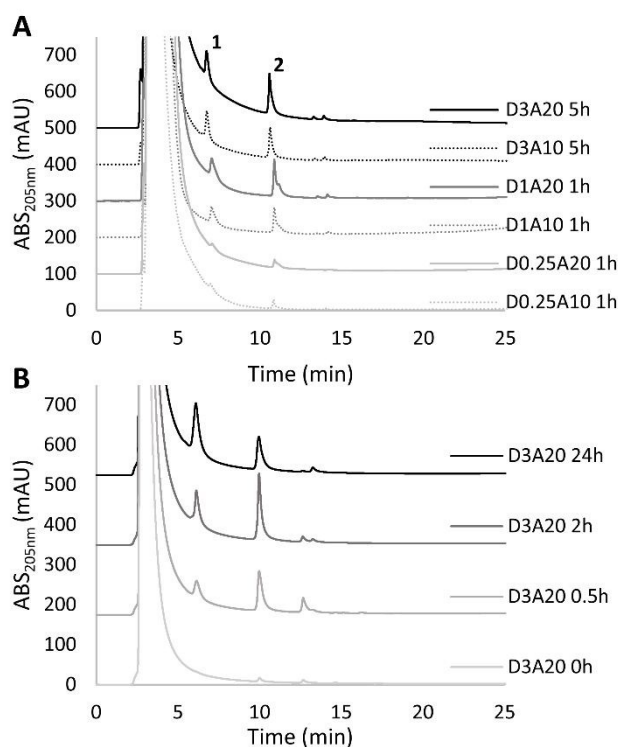


**Fig. 3. A)** Study on impact of reaction parameters with 2  $\mu$ M *TrMan5A*, LBG (0.25, 1 or 3% (w/v)) and HEMA (10 or 20 vol%). Presented HPLC chromatograms represent the incubation time required to obtain maximum peak area of M<sub>1</sub>EMA (peak 1) and M<sub>2</sub>EMA (peak 2) at the respective condition. D = donor (LBG) concentration in % (w/v), A = acceptor (HEMA) concentration (vol%). Samples of 3% (w/v) LBG reactions were diluted 1:3 with ACN, whilst all others were diluted 1:1 with ACN. **B)** Time course study on the reaction with 2  $\mu$ M *TrMan5A*, LBG (3% (w/v)) and HEMA (20 vol%), from 0-24 h. Analysis after 3x 1:1 HEMA extraction with diethyl ether (see methods section).



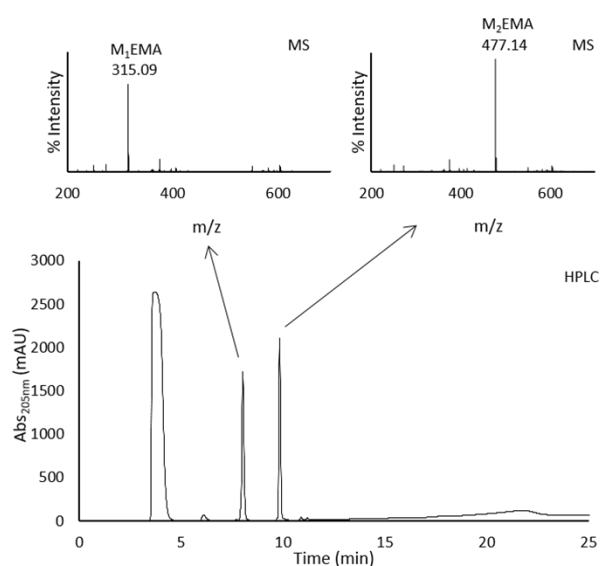


**Fig. 4.** Chromatogram of preparative HPLC purification carried out with a preparative NH<sub>2</sub> column, run under HILIC conditions. 8 ml of sample was injected during an isocratic flow of 95% ACN and 5% H<sub>2</sub>O, followed by a gradient from 95 to 40% ACN over 13 min. Two major peaks were detected after the void: *r<sub>f</sub>* 1: 8.0 min, 2: 9.9 min. Fractions were collected and the peaks were individually identified as M<sub>1</sub>EMA and M<sub>2</sub>EMA by MALDI-ToF MS. Theoretical m/z for M<sub>1</sub>EMA: 315.11 and M<sub>2</sub>EMA: 477.16.





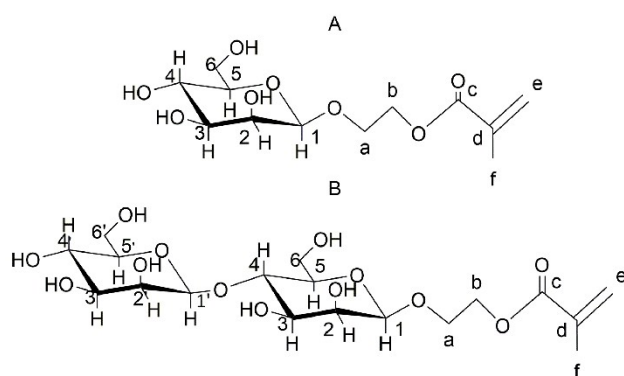


**Fig. 5.** The expected  $\beta$ -configured structures of the synthesised mannosyl acrylates. **A)**  $M_1EMA$  **B)**  $M_2EMA$ . Number 1 is assigned to the anomeric position and then following clockwise direction. For the acrylate part, carbons have been labelled a-f from the glycosidic bond oxygen.



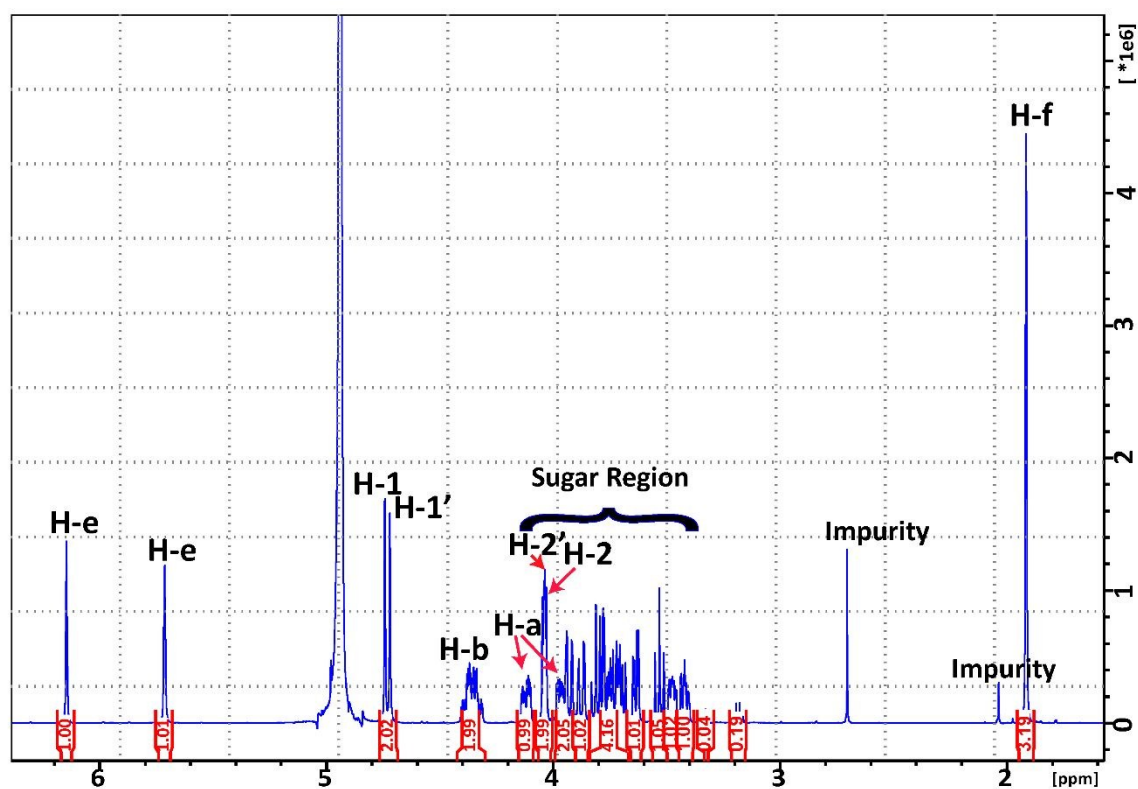
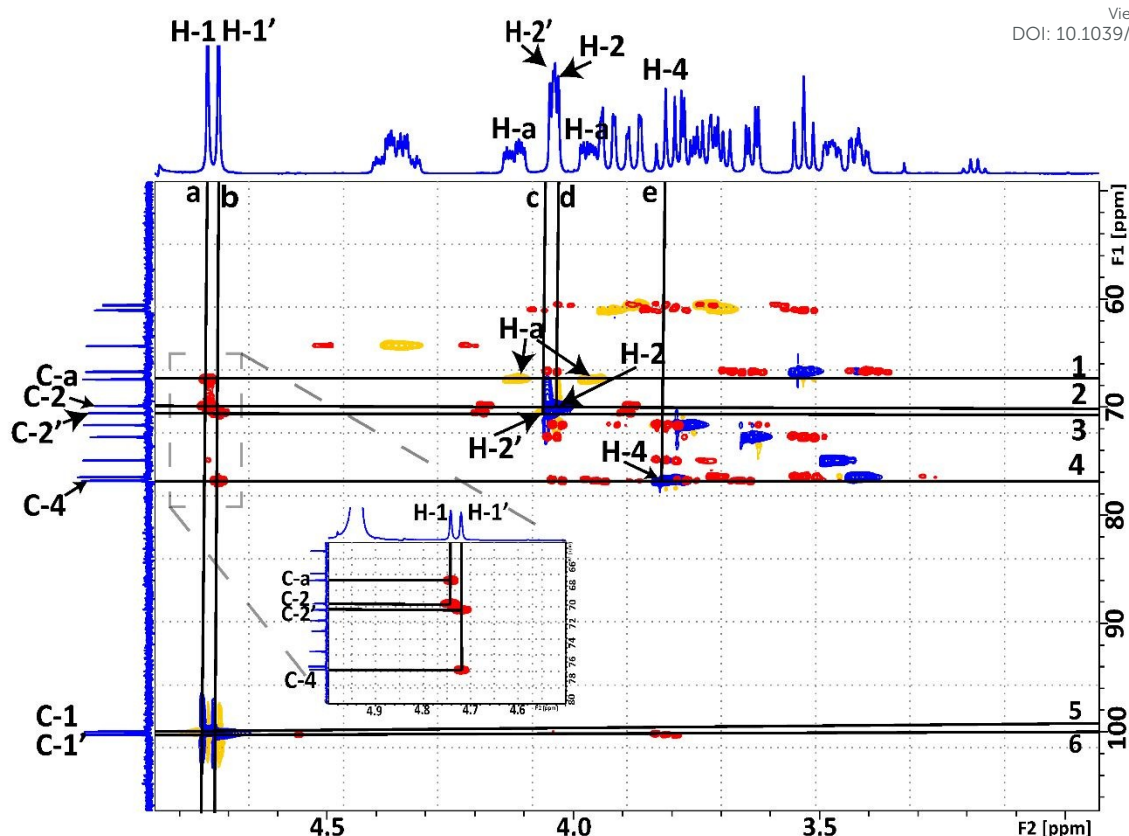
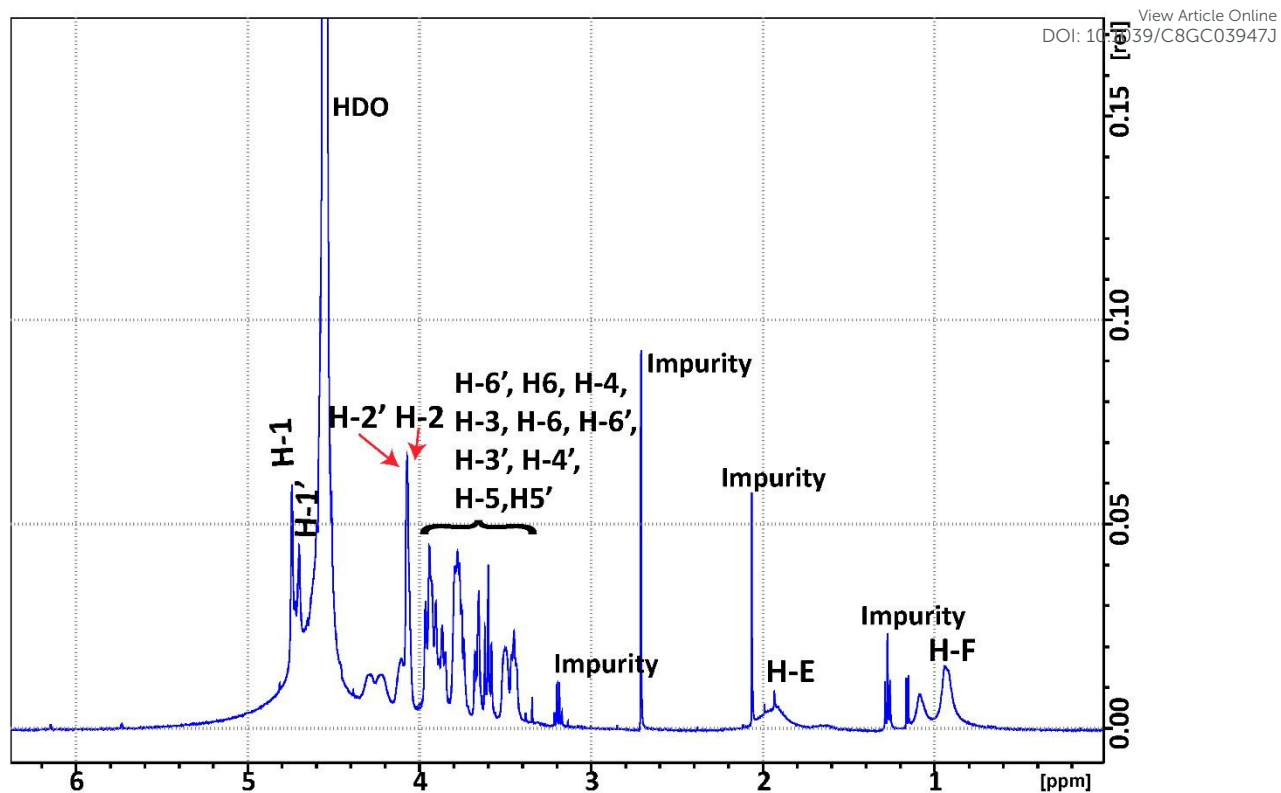


Fig. 6.  $^1\text{H}$  NMR spectrum of the synthesised  $\text{M}_2\text{EMA}$  collected at  $10^\circ\text{C}$ .



**Fig. 7.** Overlay of  $^1\text{H} - ^{13}\text{C}$  HMBC (red, positive signals) and HSQC (blue, positive signals; yellow, negative signals) NMR spectra of the synthesised  $\text{M}_2\text{EMA}$ . Chemical shifts in ppm ( $\delta$ ). The horizontal lines are drawn at (from top to bottom): **(1)**  $\delta_{\text{C}}$  67.38 of C-a, along that line direct bond J-coupling to H-a protons from crosspeak in HSQC at  $\delta_{\text{H}}$  4.12 and at  $\delta_{\text{H}}$  3.97; **(2)**  $\delta_{\text{C}}$  69.83 of C-2, along that line direct bond J-coupling to H-2 protons from crosspeak in HSQC at  $\delta_{\text{H}}$  4.03; **(3)**  $\delta_{\text{C}}$  70.5 of C-2', along that line direct bond J-coupling to H-2' protons from crosspeak in HSQC at  $\delta_{\text{H}}$  4.04; **(4)**  $\delta_{\text{C}}$  76.8 of C-4, along that line direct bond J-coupling to H-4 protons from crosspeak in HSQC at  $\delta_{\text{H}}$  3.8; **(5)**  $\delta_{\text{C}}$  99.97 of C-1 with cross peak in HSQC with the H-1 protons at  $\delta_{\text{H}}$  4.74 ppm indicating a direct bond J-coupling between C-1 and H-1; **(6)**  $\delta_{\text{C}}$  100.21 of C-1' with cross peak in HSQC with the H-1' at  $\delta_{\text{H}}$  4.72 indicating a direct bond J-coupling between C-1' and H-1'. The vertical lines are drawn at **(a)**  $\delta_{\text{H}}$  4.74 of H-1. In the **insert**, along this vertical line two long-range J-couplings to C-2 at  $\delta_{\text{C}}$  69.83 and to C-a of the acrylate at  $\delta_{\text{C}}$  67.38; **(b)**  $\delta_{\text{H}}$  4.72 of H-1' of the second mannose unit. In the insert, along this vertical line two long-range J-couplings to C-4 at  $\delta_{\text{C}}$  70.5 and to C-4' at  $\delta_{\text{C}}$  76.8; vertical lines c, d and e drawn at crossings described in horizontal lines 3, 2 and 4 respectively. All spectra collected at 10  $^{\circ}\text{C}$  in  $\text{D}_2\text{O}$ .





**Fig. 8.**  $^1\text{H}$  NMR spectrum of poly( $\text{M}_2\text{EMA}$ ) collected at  $45^\circ\text{C}$ ,  $\text{D}_2\text{O}$ . HDO – residual water peak.



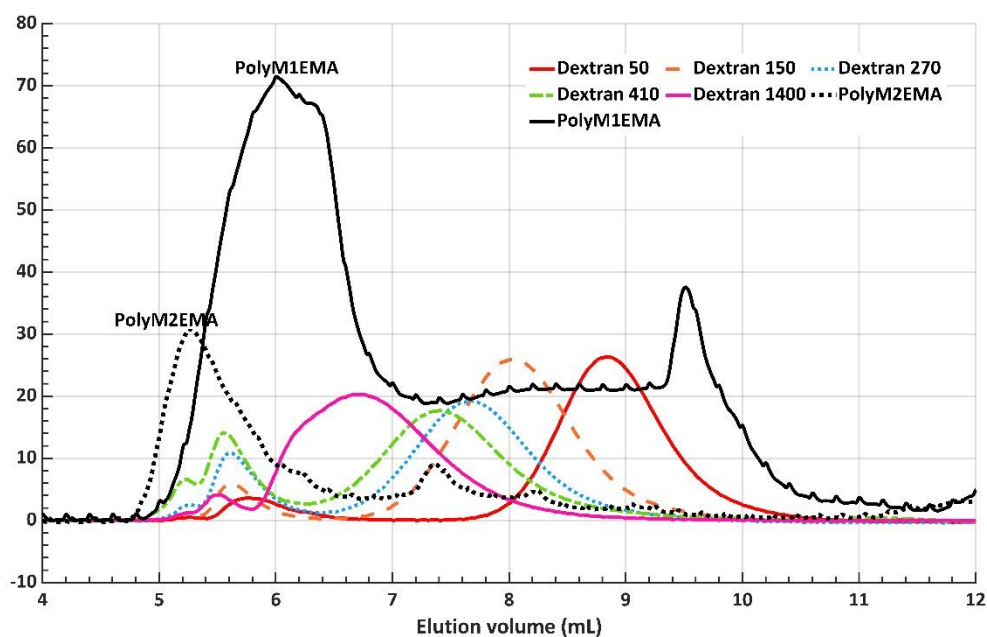


**Fig. 9.** SEC chromatogram of poly(M<sub>2</sub>EMA) and poly(M<sub>1</sub>EMA), including dextran standards (Mw 50, 150, 270, 410 and 1400 kDa). Poly(M<sub>2</sub>EMA) eluted with the void volume (5.2 ml).

